

Fast estimation of distance between two hydrophones using ocean ambient noise in multi-ship scenarios

Xuefeng Liu(刘雪枫), Zhi Xia(夏峙), Qi Li(李琪), and Ye Ding(丁烨)
Citation: Chin. Phys. B, 2023, 32 (**12**): 124301. DOI: 10.1088/1674-1056/acf91b
Journal homepage: http://cpb.iphy.ac.cn; http://iopscience.iop.org/cpb

What follows is a list of articles you may be interested in

Method for measuring the low-frequency sound power from a complex sound source based on sound-field correction in a non-anechoic tank

Hongzhe Xu(徐宏哲), Qi Li(李琪), Rui Tang(唐锐), and Dajing Shang(尚大晶)
Chin. Phys. B, 2023, 32 (**5**): 054303. DOI: 10.1088/1674-1056/acb75c

Three-dimensional acoustic propagation model for shallow waters based on an indirect boundary element method

Edmundo F. Lavia, Juan D. Gonzalez, and Silvia Blanc
Chin. Phys. B, 2023, 32 (**5**): 054301. DOI: 10.1088/1674-1056/ac90b1

Effect of porous surface layer on wave propagation in elastic cylinder immersed in fluid

Na-Na Su(苏娜娜), Qing-Bang Han(韩庆邦), Ming-Lei Shan(单鸣雷), and Cheng Yin(殷澄)
Chin. Phys. B, 2023, 32 (**1**): 014301. DOI: 10.1088/1674-1056/ac6ee6

Lamb waves topological imaging combining with Green's function retrieval theory to detect near filed defects in isotropic plates

Hui Zhang(张辉), Hai-Yan Zhang(张海燕), Meng-Yun Xu(徐梦云), Guo-Peng Fan(范国鹏), Wen-Fa Zhu(朱文发), Xiao-Dong Chai(柴晓冬)
Chin. Phys. B, 2019, 28 (**7**): 074301. DOI: 10.1088/1674-1056/28/7/074301

A passive source ranging method based on the frequency warping transform of the vertical intensity flux in shallow water

Yu-Bo Qi(戚聿波), Shi-Hong Zhou(周士弘), Meng-Xiao Yu(于梦枭), Shu-Yuan Du(杜淑媛), Mei Sun(孙梅), Ren-He Zhang(张仁和)
Chin. Phys. B, 2019, 28 (**5**): 054302. DOI: 10.1088/1674-1056/28/5/054302

Fast estimation of distance between two hydrophones using ocean ambient noise in multi-ship scenarios

Xuefeng Liu(刘雪枫)[1,2,3], Zhi Xia(夏峙)[1,2,3,†], Qi Li(李琪)[1,2,3], and Ye Ding(丁烨)[4]

[1] *National Key Laboratory of Underwater Acoustic Technology, Harbin Engineering University, Harbin* 150001, *China*
[2] *Key Laboratory of Marine Information Acquisition and Security (Harbin Engineering University), Ministry of Industry and Information Technology, Harbin* 150001, *China*
[3] *College of Underwater Acoustic Engineering, Harbin Engineering University, Harbin* 150001, *China*
[4] *Library, Harbin Engineering University, Harbin* 150001, *China*

(Received 7 June 2023; revised manuscript received 19 August 2023; accepted manuscript online 13 September 2023)

Accurately estimating the bearing of a target with two hydrophones requires knowing the precise distance between them. However, in practice, it is difficult to measure this distance accurately due to the influence of current. To solve this problem, we propose a method for extracting the time-domain Green's function between two points in multi-ship scenarios and for extracting the time-domain waveform arrival structure between two hydrophones in real-time based on long samples of ship radiation noise cross-correlation. Using the cross-correlation function of the radiated noise from any ship located in the end-fire direction of the two hydrophones, we can estimate the distance between the hydrophones in real-time. To verify the accuracy of our estimation, we compare the result of azimuth estimation with the actual azimuth based on the azimuth estimation of a cooperative sound source in the maritime environment. Our experimental results show that the proposed method correctly estimates the distance between two hydrophones that cannot be directly measured and estimates the position of a cooperative sound source 4 km away with an average deviation of less than 1.2°.

Keywords: ocean ambient noise, the time-domain Green's function, cross-correlation

PACS: 43.30.+m, 43.60.+d, 92.10.Yb, 92.10.Vz **DOI:** 10.1088/1674-1056/acf91b

1. Introduction

In the actual environment, it is difficult to accurately measure the distance between the two hydrophones due to the inevitable influence of wind, wave, surge and flow, which leads to the deviation of azimuth estimation.[1] During operation, the synchronous measurement of a sonar array is crucial to ensure accurate estimates of the target azimuth estimation results. Currently, research on this problem can be classified into two categories: active and passive methods. The basis of these methods is to measure the distance between the two hydrophones by acoustic method. The traditional active measurement method needs to use the active sound source. However, considering the multipath effect in the shallow sea environment and the interference of other irrelevant signals, it is difficult to measure accurately. The empirical Green's function method is a main method used in passive measurement methods. It does not require active sound source cooperation during use, and it is not limited by time and space. During the process, this method does not cause sound pollution and can reduce the difficulty of measurement. Additionally, it is more convenient in engineering practice.

Extracting Green's function from noise originated from seismological research.[2] Sabra and Roux *et al*. found that the time derivative of the time-domain noise cross-correlation function (NCF) is related to the time-domain Green's function (TDGF) between two points from the ocean ambient noise.[3] Then they proved this phenomenon in theory[4] and extended it to the case of homogeneous media with attenuation,[5] which greatly promoted the development of this research in the field of underwater acoustics. Godin extended this theory to the diffusion acoustic noise field in any inhomogeneous fluid[6] and used it to evaluate the velocity and sound velocity between two points.[7] Fried and Kuperman[8] extracted TDGF in the horizontal array. Since then, the research has been widely used. Siderius[9] and Harrison[10] conjectured the layered structure of the seabed. G F Li[11] and J Li[12,13] realized passive imaging of scatterers and inversion of seabed geoacoustic parameters. X L Li[14] detected quiet targets. Zhou[15] applied vector hydrophones to suppress the interference of non-stationary noise sources in the distance. Sabra[16] and Yang[17] combined the least squares method and the multi-dimensional scaling method to achieve the calibration of the formation. Tan[18,19] inverted the dispersion curve of passive measurement, and Guo[20] used the method of sub-band binary weighted accumulation to improve the signal-to-noise ratio of broadband extraction.

In many applications, the measurement of hydrophone spacing is an important parameter that directly affects the accuracy of target azimuth estimation. The TDGF between two points can be extracted by using the ocean ambient noise, and the time arrival structure between two points can be obtained.

†Corresponding author. E-mail: xz885511@hrbeu.edu.cn

© 2023 Chinese Physical Society and IOP Publishing Ltd

Then the distance information between two hydrophones can be obtained under passive conditions. However, due to the inhomogeneity of the spatial distribution of ocean ambient noise, in order to meet the requirements of the general empirical Green's function method,[21–23] a long-term cumulative signal is required. The purpose of time accumulation is that on the one hand, the inhomogeneity of spatial distribution can be compensated by multi-shot data. On the other hand, the longer the accumulation time is, the more significant the delay peak in the end-fire direction is, and the more accurate the time arrival structure is. By numerical analysis, Derode[24] pointed out that the time-domain waveform arrival structure between two hydrophones can be obtained by extracting the main features of TDGF. Roux[25] studied the problem of extracting TDGF from the radiated noise of a moving ship, and indicated that the main characteristics of TDGF between two hydrophones can be obtained by using the cross-correlation function of the ship noise, when the ship is located in the end-fire direction of the two hydrophones. Therefore, increasing the length of the signal sample for calculating the cross-correlation can highlight the cross-correlation function characteristics of the ship, when it is located in the end-fire direction of the two-hydrophone connection. The main features of TDGF are extracted by ship noise, so as to calculate the distance between two hydrophones, which is suitable for application scenarios with high real-time requirements such as target detection.

In the experiment discussed herein, two hydrophones were hoisted on the experimental platform with a cable, with no connection between them. The measured distance between the lifting points was 32.7 m. Accounting for measurement errors caused by the swing of the hanger arms and water flow, the actual distance between the two hydrophones is estimated by the method of this paper to be about 25 m. The method is applied to the two hydrophones to achieve the azimuth estimate of the cooperative sound source at a distance of 4 km, and the average deviation is less than 1.2°, which could improve the accuracy with which the azimuth of two hydrophones is estimated in real-time.

2. Theory and simulation

2.1. Basic principle of time-domain Green's function between two points for extraction of ambient noise

According to Ref. [24], when considering only absorption loss of water body for any two receiving points A and B in the underwater space and a sound source C, the cross-correlation function of the signal received at points A and B can be expressed as

$$\begin{aligned}\mathrm{Corr}_{\mathrm{AB}}(\tau) &= \int s_{\mathrm{A}}(t)\, s_{\mathrm{B}}(t+\tau)\,\mathrm{d}t \\ &= h_{\mathrm{AC}}(\tau)\otimes h_{\mathrm{BC}}(-\tau)\otimes f(\tau), \end{aligned} \tag{1}$$

where $s_{\mathrm{A}}(t)$ and $s_{\mathrm{B}}(t)$ are the receiving signals of points A and B, respectively, $h_{\mathrm{AC}}(\tau)$ and $h_{\mathrm{BC}}(\tau)$ are the impulse response functions from point A to sound source C and from point B to sound source C, respectively, and $f(\tau)$ is the autocorrelation function of the signal from sound source C. If the space is a closed and empty cavity, we have $h_{\mathrm{AC}}(\tau)\otimes h_{\mathrm{BC}}(-\tau) = h_{\mathrm{AB}}(\tau)\otimes h_{\mathrm{CC}}(-\tau)$; thus, equation (1) can be rewritten as

$$\mathrm{Corr}_{\mathrm{AB}}(\tau) = h_{\mathrm{AB}}(\tau)\otimes h_{\mathrm{CC}}(-\tau)\otimes f(\tau). \tag{2}$$

The TDGF between two points represents the impulse response between them. Equation (2) shows that the cross-correlation function of the received signal between points A and B in a closed cavity can recover the TDGF between two points.

When the sound source C is a group of coherent noise sources evenly distributed on a plane that completely encompasses the receiving points A and B, then there is a relationship between the receiving points A, B, and such a group of sound sources:

$$\sum_{\mathrm{C}} h_{\mathrm{AC}}(-\tau)\otimes h_{\mathrm{CB}}(\tau) = h_{\mathrm{BA}}(\tau) + h_{\mathrm{BA}}(-\tau). \tag{3}$$

Assuming that the transmission path between any two points I and J in the underwater space is completely reversible, that is $h_{\mathrm{IJ}}(\tau) = h_{\mathrm{JI}}(\tau)$, sound waves can propagate in both directions without loss of information. The combination of Eqs. (1) and (3) shows that, by averaging the cross-correlation function of the signals received at points A and B from each sound source, it is also possible to restore the time-domain Green's function between points of A and B. However, the accuracy of the recovery is proportional to the number of sound sources.

2.2. Theoretical model of TDGF between two points considering ship-radiated noise extraction

It is found that the existing ocean ambient noise models only consider the uniform distribution of noise sources on the ocean surface. However, the models do not cover the impact of many unevenly distributed ship-radiated noises nearby.

The cross-correlation function of the two receiving points calculated by the K/I ocean ambient noise field model proposed by Kuperman[26] is as follows:

$$\begin{aligned} C_{\omega}(R,z_1,z_2) = {} & \frac{\pi Q_1^2(\omega)}{4\rho^2(z')k^2(\omega)} \sum_n \psi_n(z_1)\psi_n(z_2)\frac{\psi_n^2(z')}{\alpha_n K_n} \\ & \times \left[\mathrm{H}_0^{(1)}(k_n R) - \mathrm{H}_0^{(1)}(k_n^* R)\right], \end{aligned} \tag{4}$$

where $Q_1(\omega)$ is the power spectrum of the sea surface noise source, α_n is the imaginary part of the eigenvalue, K_n is the real part of the eigenvalue, $\psi_{n,m}(z)$ is the normal wave eigenfunction, $k_{n,m}$ is the eigenvalue, z' is the noise source depth, $\rho(z')$ is the density, and $k(\omega)$ is the wave number.

To address this limitation, we introduce the influence of ship-radiated noise sources. We consider two receiving points, denoted as R_1 and R_2, which are located at horizontal distances from the ship noise source. The noise field at points (r_1,z_1), (r_2,z_2) can be expressed as follows:

$$\phi(r_1,z_1) = S_1(r)g(r_1,r,z_1,z), \tag{5}$$

$$\phi(r_2,z_2) = S_1(r)g(r_2,r,z_2,z). \tag{6}$$

In the above equations, $g(r_1,r',z_1,z')$, $g(r_2,r'',z_2,z')$ are the Green's functions, and S_1 is the noise source level of the ship-radiated noise.

The Green's function of the point source sound pressure can be expressed as the sum of the normal modes of each order.

$$g(\boldsymbol{r}',z_1,z) = \frac{\mathrm{i}}{4\rho}\sum_n \psi_n(z_1)\psi_n(z)\mathrm{H}_0^{(1)}(k_n\boldsymbol{r}'). \tag{7}$$

According to this, the ship radiated noise field can be calculated, the cross-correlation function of the two receiving points can be expressed as

$$C_\omega(r_1,r_2,z_1,z_2) = S_1(r)S_1^*(r)g(r_1,r,z_1,z)g^*(r_2,r,z_2,z). \tag{8}$$

Letting $R \equiv r_1 - r_2$, we get

$$C_\omega(R,z_1,z_2) = \frac{Q_2^2(\omega)}{16\rho^2(z')}\sum_m\sum_n \psi_n(z_1)\psi_m(z_2)\psi_n(z')\psi_m(z') \times \mathrm{H}_0^{(1)}(k_nR_1)\mathrm{H}_0^{(1)}(-k_mR_2), \tag{9}$$

where $Q_2(\omega)$ is the power spectrum of the ship-radiated noise.

In addition, when considering the multi-ship scene in an actual environment, numerous ship trajectories pass through the end-fire direction of the two receiving points. Equation (9) is integrated along a ship trajectory of length L. The average of the results after integration can be obtained as follows:

$$\langle C_\omega(R,z_1,z_2)\rangle = \frac{Q_1^2(\omega)}{16\rho^2(z')}\sum_m\sum_n \psi_n(z_1)\psi_m(z_2)\psi_n(z')\psi_m(z')\frac{2}{L} \times \int_0^{L/2}\mathrm{H}_0^{(1)}(k_nR_1)\mathrm{H}_0^{(1)}(-k_mR_2)\,\mathrm{d}^2R_2. \tag{10}$$

The integral part of Hankel function is calculated separately. By using the properties of Hankel function, it can be obtained as follows:

$$F_{mn} = \frac{2}{L}\int_0^{L/2}\mathrm{H}_0^{(1)}(k_nR_1)\mathrm{H}_0^{(1)}(-k_mR_2)\,\mathrm{d}^2R_2 = \frac{2}{L}\left[\frac{k_mR_2\mathrm{H}_0^{(1)}(k_nR_1)\mathrm{H}_{-1}^{(2)}(k_mR_2) - k_nR_1\mathrm{H}_{-1}^{(1)}(k_nR_1)\mathrm{H}_0^{(2)}(k_mR_2)}{k_n^2-k_m^2}\right]_0^{L/2}. \tag{11}$$

When the ship is located in the end-fire direction of the two receiving points, we can get $|R_1 - R_2| = R$. Substituting it into Eq. (11), it can be obtained that after separation and simplification

$$F_{mn} = \frac{\sin((k_n-k_m)\frac{L}{2})}{(k_n-k_m)\frac{L}{2}}\frac{\mathrm{H}_0^{(1)}(k_nR)}{\sqrt{k_m}}. \tag{12}$$

We have

$$f_{mn} = \frac{\sin((k_n-k_m)\frac{L}{2})}{(k_n-k_m)\frac{L}{2}},$$

when it satisfied $L \gg 1/\min_{n,m}(k_n-k_m)$,

$$f_{mn} = \begin{cases} 0, & m \neq n, \\ 1, & m = n. \end{cases} \tag{13}$$

After normalizing the cumulative average of the multi-ship trajectory integration results, the cross-correlation function is extended to the multi-ship scene

$$\langle C_\omega(R,z_1,z_2)\rangle = \frac{Q_1^2(\omega)}{16\rho^2(z')}\sum_n \psi_n(z_1)\psi_n(z_2) \times \frac{\psi_n^2(z')}{\sqrt{k_n}}\mathrm{H}_0^{(1)}(k_nR). \tag{14}$$

It can be observed that the cross-correlation function derived in the multi-ship scenario has a structure similar to that of surface sound sources. Through cumulative averaging of multi-ship scenarios, the correlation function after averaging can compensate for the contingency of ship-radiated noise, thereby supplementing the far and near ship-radiated noise.

2.3. Simulation of TDGF theoretical model between two points for ship-radiated noise extraction

A shallow ocean ambient is simulated under the condition of simulation experiment. The environmental parameters are depicted in the Fig. 1. The sea depth is 46 m, the sound velocity in seawater is 1500 m/s, and the density is 1 g/cm^3. The sound speed profile is uniform throughout the water column. The seabed is a semi-infinite space covered with a layer of sedimentary material 20-m thick. The sound velocity of the sedimentary layer is 1600 m/s, and its density is 1.8 g/cm^3. The seabed attenuation coefficient is 0.45 dB/λ. The noise source is a point source uniformly distributed on an infinite plane parallel to the sea surface at a depth of 0.1 m. The simulated frequency range is 100 Hz to 1500 Hz.

First, in the ocean ambient sound field depicted in Fig. 1, a simulation of the traditional model is performed under surface sound source conditions. A hydrophone is placed at a depth of $z_1 = 24$ m, and a vertical receiving array is positioned at a horizontal interval of $R = 32.7$ m, extending from the sea

surface to the seabed. The depth of the hydrophone in the vertical receiving array is set to z_2. Using Eq. (4), the cross-spectral density of the hydrophone and each hydrophone on the vertical receiving array is calculated under surface sound source conditions, and the correlation function of the two receiving points is obtained by inverse Fourier transform to restore the time-domain arrival structure, as shown in Fig. 2(a). Equation (7) gives the expression of the Green's function, the inverse Fourier transform of the Green's function between two points is used as a comparison, as shown in Fig. 2(b).

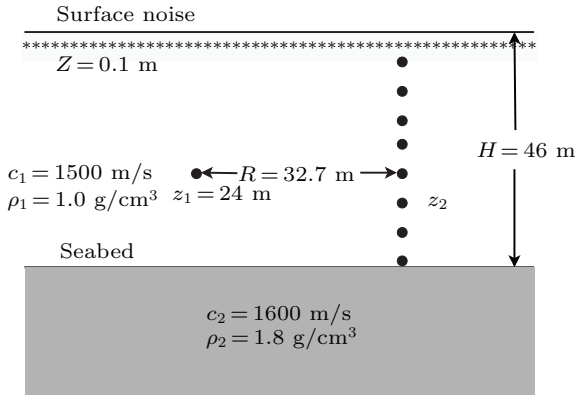


Fig. 1. Diagram of simulation environment.

Secondly, the ship-radiated noise sources are simulated in the same ocean sound field environment as shown in Fig. 1. By averaging the integral normalization of ship's trajectory, the cross-spectral density expression between the two points is calculated by Eq. (14) with considering the ship-radiated noise source. Then, the cross-spectral density of the reference hydrophone and each hydrophone on the vertical receiving array is calculated respectively, and the correlation function of the two receiving points is obtained by inverse Fourier transform. Finally, the time domain arrival structure can be restored, as shown in Fig. 2(c).

Comparing Figs. 2(a) and 2(b), it can be seen that the Green's function between the two points is basically consistent with the time arrival structure under the surface sound source model. However, when the two receiving points are at a depth of 24 m, the arrival structure of both has a certain degree of bending, which deviates from the true value. By comparing Figs. 2(a)–2(c), it can be found that the ship-radiated noise source model is basically consistent with the time arrival structure of the former two at a depth of 24-m except for the two receiving points. However, at the depth of 24 m at both receiving points, there is no bending, and it is restored to near the true value. This suggests that when a large number of ships near the two receiving points pass through the end-fire direction of the two receiving points, after the integral average normalization of the ship's trajectory, the accuracy of the time arrival structure of the two receiving points at the same depth using the ocean ambient noise calculation is improved.

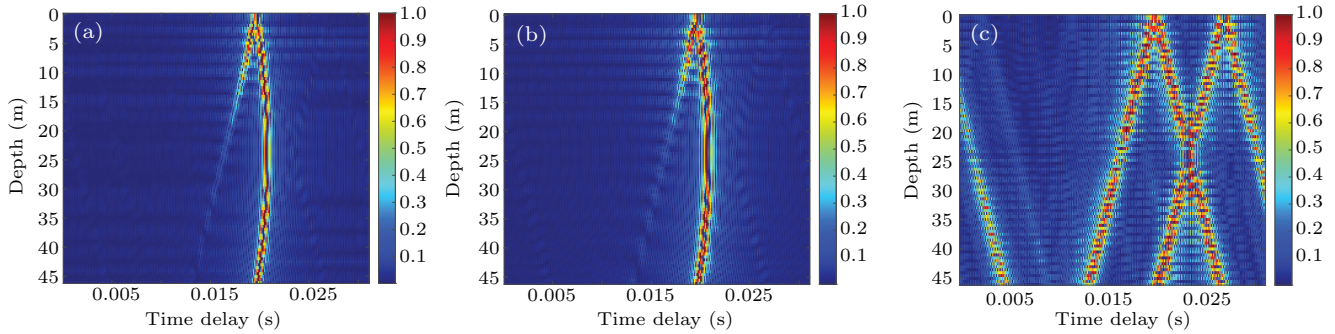


Fig. 2. Comparison of traditional surface source model, Green's function, and ship-radiated noise model in the same ocean ambient: (a) surface source, (b) Green's function, and (c) ship-radiated noise.

2.4. Fast method for extracting main features of TDGF

According to a literature analysis, estimating the distance between two hydrophones without further in-depth analysis requires only extracting the main characteristics of the TDGF between the two hydrophones. The most direct way to achieve this is to arrange a broadband transmitting transducer in the end-fire direction of the two hydrophones and calculate the distance between them through the cross-correlation of the received signals of the two hydrophones. If a ship is located in the end-fire direction of the two hydrophones, the distance can also be calculated based on the cross-correlation of the radiated noise of the ship. However, laying the required cooperative sound source or cooperative ship as discussed above is not feasible in most passive-sonar working scenarios.

In the multi-ship scenario, there is a situation where the ship sails around the two hydrophones, and the ship's motion will cause changes in the correlation of the received signals of the two hydrophones. When the ship is located in the end-fire direction of the two hydrophones, the correlation between the received signals of hydrophone varies slightly with the ship's movement. And the cross-correlation coefficient remains high under long sample cross-correlation. When the ship's azimuth is closer to the abeam direction of the two hydrophones, the ship's movement leads to a faster weakening of the correla-

tion between the signals received by the hydrophone, which is reflected in the decrease in the cross-correlation coefficient of the long sample. Therefore, through the processing method of long sample cross-correlation, the cross-correlation function of ship-radiated noise can be filtered out from the signal processing results of the hydrophone when the ship is just in the end-fire direction of the two hydrophones, and the time-domain waveform between the two hydrophones can be obtained to calculate the distance between the two hydrophones.

Let $B(\theta,\theta_0)$ be the change in the correlation coefficient of the two-hydrophone signal caused by the ship sailing from azimuth θ_0 to azimuth θ. In Fig. 3(a), the schematic diagrams of the end-fire direction, the abeam direction, and the non-end-fire direction are given by the horizontal top–down diagram. According to the derivation of $B(\theta,\theta_0)$ in Ref. [25], when the ship is located in the end-fire direction of the two hydrophones, the change in correlation of the two hydrophones caused by the ship motion is given by

$$B(\delta\theta,0)=B(\delta\theta,\pi)\simeq 1-\frac{\delta\theta^4}{8}\left(\frac{R}{c}\right)^2\left(\omega^2+\frac{\Delta\omega^2}{12}\right), \quad (15)$$

where $\delta\theta \ll \theta_0$ is the small change in ship azimuth caused by the ship motion.

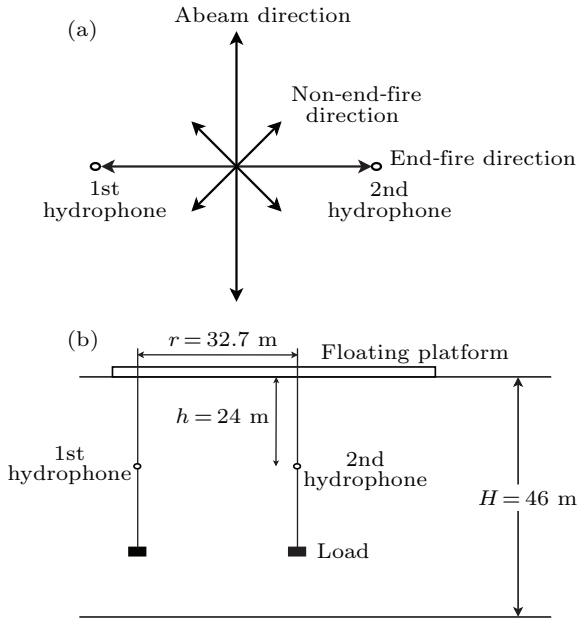


Fig. 3. (a) Horizontal top–down diagram, (b) layout of experimental offshore hydrophone.

When the ship is located in the non-end-fire direction of the two hydrophones, we get

$$B(\theta_0+\delta\theta,\pi)\simeq 1-\frac{\delta\theta^2}{2}\left[\frac{2R\sin(\theta_0)}{c}\right]^2\left(\omega^2+\frac{\Delta\omega^2}{12}\right). \quad (16)$$

According to the calculation results of Ref. [25], the ratio of normalized Eq. (15) to Eq. (16) can reach up to 25 dB, which is basically consistent with the experimental results. It can be verified that when the ship is located in the end-fire direction of the two hydrophones, the effect of Green's function extraction is better than that in the non-end-fire direction. In Fig. 2(c), the time domain arrival structure between two points can be accurately obtained in the end-fire direction, but there is a large interference in the non-end-fire direction. However, the difference between the end-fire direction and the non-end-fire direction is not seen in Figs. 2(a) and 2(b).

On October, 2018, the sea experiment was conducted in the Yellow Sea, approximately 50-km southeast of Shidao, Shandong Province. The water depth of the experimental area was approximately 46 m, and the sea state was about 1–2 levels. The sound velocity profile of the seawater changed gradually, and there was no evident thermocline, approximated at 1500 m/s. The two hydrophones were hung on the same side and fixed under a floating metal platform. There were 150 kg of weights hanging below to ensure that the two hydrophones were approximately horizontal underwater. The depth direction of the two hydrophones was about 24 m below sea level. The vertical slice diagram is shown in Fig. 3(b).

The data preprocessing involves several steps: trend term removal, mean value, normalization, band-pass filtering, and whitening processing. The resulting preprocessed signal is utilized for cross-correlation processing, and the cross-correlation results are averaged multiple times to obtain a single output result. Finally, the time history of the cross-correlation function is normalized. Figure 4 shows the processing flow.

In the data preprocessing, removing the detrend item can eliminate the influence of the offset generated by the receiver when obtaining data on the later calculation. The mean removal makes each dimension of the input data centralize to 0. The band-pass filter separates the data with an analysis bandwidth of 500 Hz–1000 Hz. The purpose of whitening is to remove the correlation between data and homogenize the variance. After data preprocessing, the analysis can be concentrated on the fluctuation of the data trend itself, and the effect has been better improved. Figure 5 shows the effect of data preprocessing on the results of Green's function extraction.

Comparing Figs. 5(a) and 5(b), it can be seen that due to the large interference of the original data, there will be relatively strong interference at the time domain arrival structure, and the accurate Green's function cannot be extracted. After data preprocessing, the analysis can be focused on the fluctuation of the data trend itself, which significantly improves the extraction effect of the Green's function. By comparing Figs. 5(b)–5(d), it can be seen that the extraction effect of Green's function is obviously improved with the increase of sample lengths, and the side lobes near the time domain arrival structure are gradually reduced.

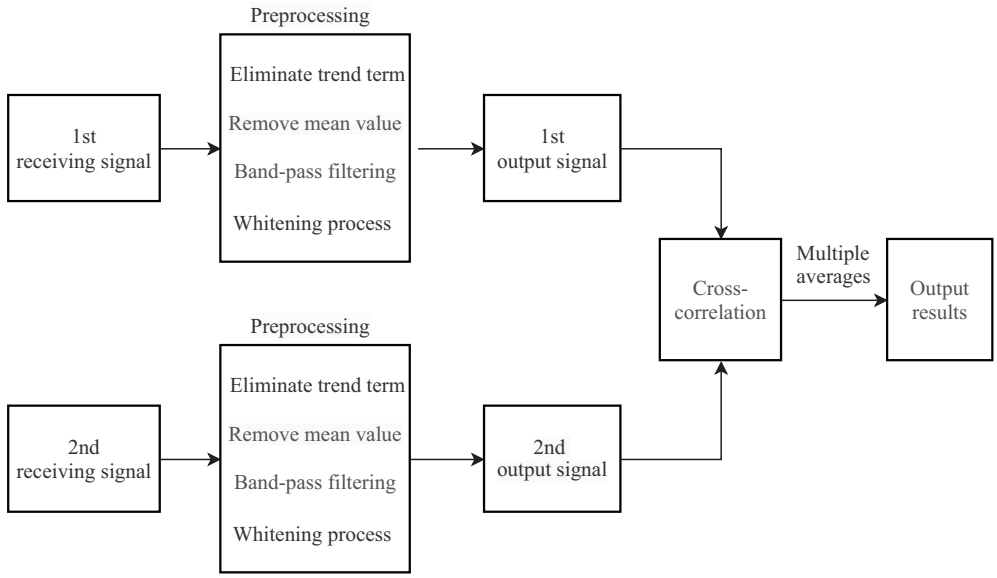


Fig. 4. Diagram of data processing flow.

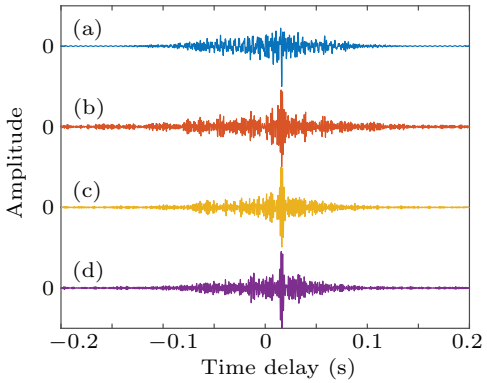


Fig. 5. The effect of extracting Green's function under different processing conditions (a) The sample length without data preprocessing is 5 s. (b)–(d) The sample lengths after data preprocessing are 5 s, 30 s, 60 s, respectively.

Based on the signal received by the AIS receiver installed on the experimental platform, several ships are present within 50 km of the experimental platform, distributed as shown in Fig. 6. The figure shows the experimental platform as the central dot and the position of the ships obtained from the AIS data as triangles.

According to the AIS data collected in the experiment, the 20-minute data of a cargo ship sailing around the experimental platform were selected for analyses. And the cross-correlation processing was performed on sample lengths of 5 s, 30 s, and 60 s. Figure 7 shows the resulting normalized time history diagram.

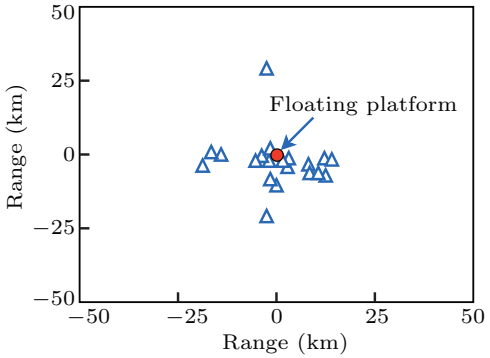


Fig. 6. Ship distribution on the sea surface when the cooperative sound source transmits signal.

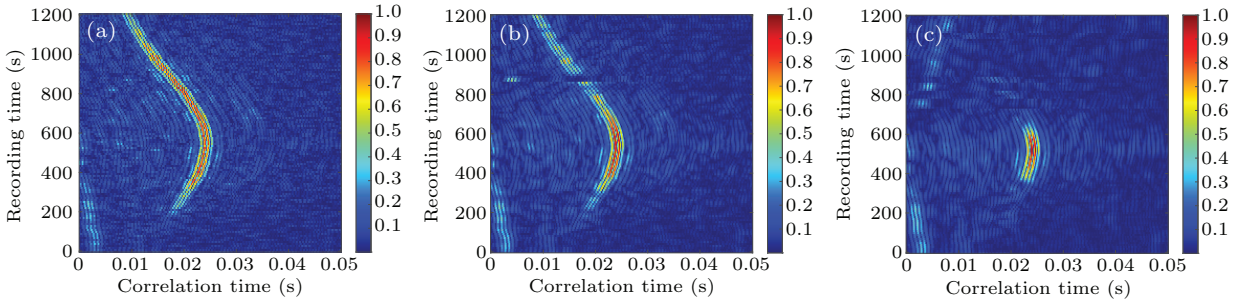


Fig. 7. Normalized time history of the cross-correlation function of two-hydrophone signals when a ship target sails around the experimental platform: (a) sample length of 5 s, (b) sample length of 30 s, and (c) sample length of 60 s.

Figure 7 shows that the correlation of ship-radiated noise between two hydrophones and the ship azimuth change is consistent with the above analyses. The normalized time history diagram of the cross-correlation function of the long sample has distinct features only when the ship is situated in the end-fire direction of the two-hydrophone connection, and these

features weaken when the ship is oriented in other directions. This characteristic reveals the time-domain waveform arrival structure between the two hydrophones, which can be used to estimate the distance between them. Compared with the traditional empirical Green's function extraction method, this method can estimate the distance between two hydrophones in near-real-time in a multi-ship scenario, without requiring long-term cumulative averaging of the cross-correlation function of ambient noise.

2.5. Experimental verification of marine cooperative sound source

This part does not aim to use a cooperative sound source for measuring the distance between the two hydrophones directly, as such a kind of active measurement would lead to significant errors compared with the real value. Instead, we adopt the passive method, using the distance between the two hydrophones measured by the ship-radiated noise source in the ocean ambient to estimate the target azimuth of the cooperating sound source. Next, the target azimuth measured by the distance between the two hydrophones is compared with the actual results from the target azimuth. Hence, the accuracy of the distance between the two hydrophones would be verified.

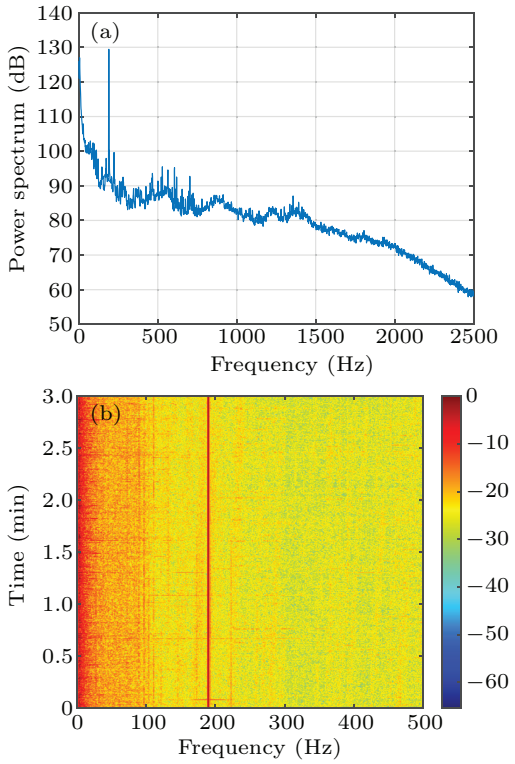


Fig. 8. Analysis of received signal when the cooperative sound source transmits single-frequency signal (a) power spectrum of received signal and (b) LOFAR diagram of received signal.

One subject of the experiment involves bearing estimation of the cooperative sound source at sea. A launching ship carries the cooperative sound source and emits a single-frequency signal of 190 Hz at a distance of about 4 km from the real platform. The experimental system's sampling frequency is 5 kHz. The sound source emits a continuous 190-Hz single-frequency signal, and we selected 3 min of data from the received signal for analyses. Figure 8 shows the power spectrum and LOFAR results, respectively.

Based on the distance measured between the two hydrophones shown in Fig. 8, the cross-spectral phase comparison method was used to calculate the azimuth of the cooperative sound source, which was then compared with the true value of the cooperative sound source azimuth calculated by the GPS carried by the launch ship. The results are presented in Fig. 9.

Figure 9 reveals a significant difference between the estimated value and the true value of the azimuth of the cooperative sound source. We conclude that the direction-finding task of the cooperative sound source cannot be completed based on the measured value of the two-hydrophone distance. One reason for this problem is that a cable suspends the two hydrophones, and there is no rigid connection between them. Under the influence of water flow, the actual distance between the two hydrophones and the measured value of the lifting point have changed significantly. Therefore, the measured value of the lifting point cannot be used as the distance between the hydrophones when estimating the sound source orientation.

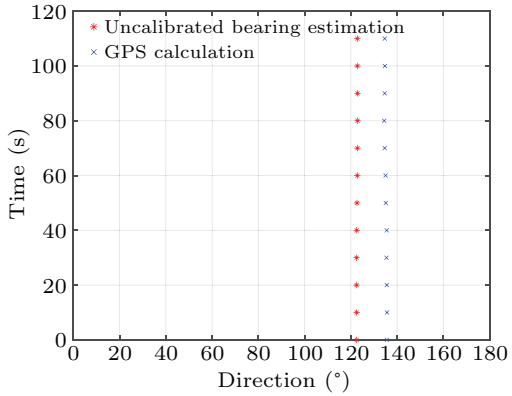


Fig. 9. Cooperative sound source azimuth estimated based on the measured value of the deployment point compared with its true value.

According to the processing flow shown in Fig. 4, the received signal of the hydrophone is processed, and a time history analysis of the cross-correlation function of the received signal of the two hydrophones is performed. To analyze the results more intuitively, the pseudo-color image, similar to Fig. 7, is binarized, and only the peak points higher than 0.6 after normalization of the cross-correlation function are extracted. The binarized time history diagram is shown in Fig. 10.

Based on Fig. 10, a nearly continuous line is observed at approximately 0.015 s. As per the previous analyses, the correlation characteristics of the moving ship in the end-fire direction of the two hydrophones are the most significant, and

the distance between the hydrophones will not change drastically in a short period. The time-domain waveform arrival structure between the two hydrophones, extracted by any ship sailing in the end-fire direction of the two hydrophones, is consistent. Thus, the distance between the hydrophones during the observation time can be estimated based on the line characteristics shown in the figure. The results are illustrated in Fig. 11 and differ significantly from the measurement results of the hydrophones.

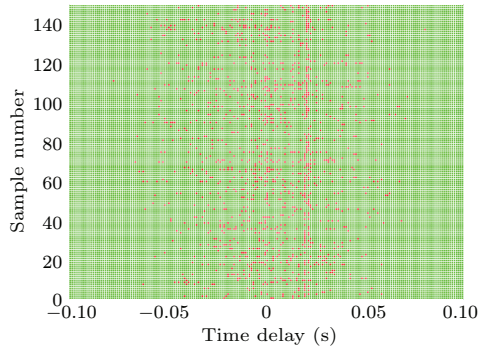


Fig. 10. Binarization time history of normalized cross-correlation function of two-hydrophone signals.

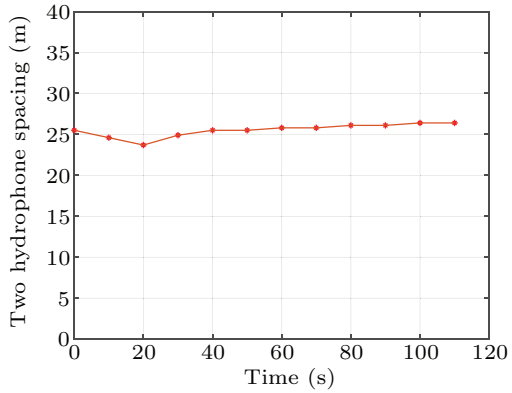


Fig. 11. Change in array distance of two hydrophones over a duration of 110 s.

To verify the accuracy of the aforementioned estimation results for the two-hydrophone distance, the azimuth of the cooperative sound source was estimated based on these results. The corresponding outcomes are presented in Fig. 12.

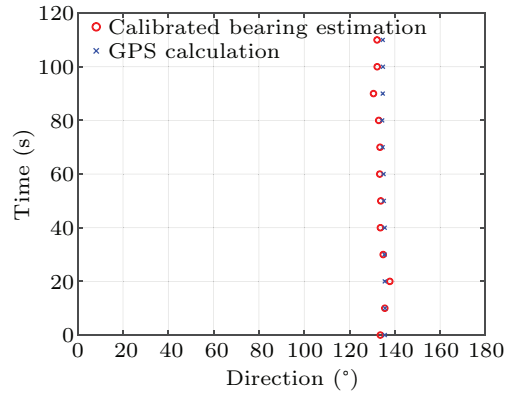


Fig. 12. Cooperative sound source azimuth calculated from the estimated distance between the two hydrophones compared with its true value.

Figure 12 shows that the azimuth of the cooperative sound source can be accurately estimated based on the estimated value of the two-hydrophone distance. The average deviation from the true value of the sound source azimuth is less than 1.2°, indicating the accuracy of the two-hydrophone distance estimated by this method.

3. Conclusion

This paper addresses the issue of estimating the distance between two hydrophones. To achieve this, a theoretical model is established for extracting the TDGF between two points in a multi-ship scenario, and a method is proposed for extracting the time-domain waveform arrival structure between two hydrophones using ship-radiated noise in a similar scenario. The method employs long sample cross-correlation processing to extract the cross-correlation characteristics of ship-radiated noise when any ship is located in the end-fire direction of the two hydrophones from the time history diagram of the received signal cross-correlation of the two hydrophones. Subsequently, the time-domain waveform arrival structure between the two hydrophones is obtained, and the distance between them is calculated. Compared with other methods that use the cross-correlation function of ocean ambient noise to extract the empirical Green's function between two hydrophones over a long time, the proposed method has the advantage of achieving near real-time distance estimation and being more suitable for specific underwater acoustic detection engineering applications. The results of the sea experiment also demonstrate the effectiveness of the proposed method in solving the real-time estimation of the distance between two hydrophones. The next key area of this research is to expand the universality of noise sources.

Acknowledgements

The authors would like to thank the captain and crew for assistance with data collection. Project supported by the National Natural Science Foundation of China (Grant No. 62171148).

References

[1] Schmudt R O 1986 *IEEE Trans. Antennas Propag.* **34** 276
[2] Claerbout and Jon F 1968 *Geophysics* **33** 264
[3] Roux P, Kuperman W A and Group N 2004 *J. Acoust. Soc. Am.* **116** 1995
[4] Sabra K G, Roux P and Kuperman W A 2005 *J. Acoust. Soc. Am.* **117** 164
[5] Roux P, Sabra K G, Kuperman W A and Roux A 2005 *J. Acoust. Soc. Am.* **117** 79
[6] Godin O A 2006 *Phys. Rev. Lett.* **97** 054301
[7] Godin O A 2012 *Acoust. Phys.* **58** 129
[8] Fried S E, Kuperman W A, Sabra K G and Roux P 2008 *J. Acoust. Soc. Am.* **124** EL183
[9] Siderius M, Harrison C H and Porter M B 2006 *J. Acoust. Soc. Am.* **120** 1315
[10] Harrison C H and Siderius M 2008 *J. Acoust. Soc. Am.* **123** 1282

[11] Li G F, Li J, Gao D Z and Wang N 2016 *Acta Acustica* **41** 49 (in Chinese)
[12] Li J, Gerstoft P, Siderius M and Fan J 2020 *J. Acoust. Soc. Am.* **148** 3836
[13] Li J, Li G F, Gao D Z and Wang N 2017 *Acta Acustica* **42** 143 (in Chinese)
[14] Li X L, Gao D Z, Li J, Li G F and Wang N 2018 *Appl. Acoust.* **37** 636 (in Chinese)
[15] Zhou J B, Piao S C, Liu Y Q, Zhang H G, Qu K, Li X M and Zhang M H 2019 *Acta Acustica* **44** 337 (in Chinese)
[16] Sabra K G, Roux P, Thode A M, D'Spain G L, Hodgkiss W S and Kuperman W A 2005 *IEEE J. Ocean. Eng.* **30** 338
[17] Yang X S, Li F H and Wang H Z 2021 *Acta Acustica* **46** 863 (in Chinese)
[18] Tan T W, Godin O A, Brown M G and Zabotin N A 2019 *J. Acoust. Soc. Am.* **146** 2321
[19] Tan T W and Godin O A 2021 *J. Acoust. Soc. Am.* **150** 2717
[20] Guo Q C, Li F H and Yang X S 2022 *Appl. Acoust.* **41** 70 (in Chinese)
[21] Lobkis O I and Weaver R L 2001 *J. Acoust. Soc. Am.* **110** 3011
[22] Weaver R L and Lobkis O I 2002 *Ultrasonics* **40** 435
[23] Weaver R L and Lobkis O I 2001 *Phys. Rev. Lett.* **87** 134301
[24] Derode A, Larose E, Tanter M, De Rosny J, Tourin A, Campillo M and Fink M 2003 *J. Acoust. Soc. Am.* **113** 2973
[25] Roux P, Kuperman W A and Group N 2004 *J. Acoust. Soc. Am.* **116** 1995
[26] Kuperman W A and Ingenito F 1980 *J. Acoust. Soc. Am.* **67** 1988